An-Najah National University

Faculty of Graduate Studies

The Magnetization of Single GaAs Quantum Dot with Gaussian Confinement

By

Mahmoud Majed Mahmoud Ali

Supervisor

Prof. Mohammad Elsaid

This Thesis is Submitted in Partial Fulfillment of the Requirements for the Degree of Master of Physics, Faculty of Graduate Studies, An-Najah National University, Nablus, Palestine.

2017

The Magnetization of Single GaAs Quantum Dot with Gaussian Confinement

By

Mahmoud Majed Mahmoud Ali

This Thesis was defended successfully on 5/10/2017 and approved by:

Defense committee members	Signature
– Prof. Mohammed Khalil Elsaid / Supervisor	.....
– Dr. Muayad Abu Saa / External examiner	.....
– Dr. Musa El Hassan / Internal examiner	.....

Dedication

For my father and my mother and my dear family for their love and support.

For my wonderful friends Izz al-Din Hassan, Hassan Hassan, Basman Odeh, Baha Hamad, Ayham Shaer, Omar Salem, Ali Mana and Mohammad Hassan for their support, love and encouragement.

Acknowledgments

I would like to express my sincere thanks to my supervisor and instructor Prof. Mohammad Elsaid for his guidance, assistance, supervision and contribution of valuable suggestions. I can't forget to thank my dear friend Ayham Shaer for his help and experience especially in Mathematica. I also thank my respected colleague Weam Obaidy for her help. Finally, I would like to thank all friends for providing encouragement and support.

الإقرار

أنا الموقع أدناه مقدم الأطروحة التي تحمل عنوان

The Magnetization of Single GaAs Quantum Dot with Gaussian Confinement

أقر بأن ما اشتملت عليه هذه الرسالة إنما هو نتاج جهدي الخاص، باستثناء ما تمت الإشارة إليه حيثما ورد، وأن هذه الرسالة ككل أو جزء منها لم يقدم من قبل لنيل أية درجة أو بحث علمي أو بحثي لدى أية مؤسسة تعليمية أو بحثية أخرى

Declaration

The work provided in this thesis, unless otherwise referenced, is the researcher's own work, and has not been submitted elsewhere for any other degree or qualification.

Student's name: **اسم الطالب :**

Signature: **التوقيع:**

Date: **التاريخ:**

Table of Contents

List of Tables

List of Figures

List of Symbols and Abbreviations

QD	Quantum dot
GQD	Gaussian quantum dot
PQD	Parabolic quantum dot
3D	Three dimension
2D	Two dimension
1D	One dimension
0D	Zero dimension (quantum dot)
$\mathcal{M}$	Magnetization
C_v	Heat capacity at constant volume
I	Current
A	Ampere
pA	Pico ampere
V_{SD}	Source-Drain voltage
V_g	Gate voltage
ω_o	Confining frequency
ω_c	Cyclotron frequency
B	Magnetic field
χ	Magnetic susceptibility
MBE	Molecular beam epitaxy
n- AlGaAs	n- type Aluminum Gallium Arsenide
2DEG	Two dimensional electron gas
e	Charge of electron
m_0	Mass of electron
m^*	Effective mass of electron
$\vec{P}(r)$	The linear momentum
$\vec{A}(r)$	Vector potential
C	Speed of light
ϵ	The dielectric constant of material
R^*	Effective Rydberg energy unit
$\hbar$	Reduced Blank's constant
i	Imaginary number
Ψ	Wave function
K	Kelvin Degree
T	Temperature
N	Principle quantum number
M	Angular quantum number
S	Spin quantum number
a^*	Effective Bohr radius

R	Quantum dot size
V_0	The depth of the confining potential
g*	The effective Lande-g factor

XIII

The Magnetization of Single GaAs Quantum Dot with Gaussian Confinement

By
Mahmoud Majed Mahmoud Ali
Supervisor
Prof. Mohammad Elsaid

Abstract

The Magnetization of single electron confined in a quantum dot presented in a magnetic field had been calculated by solving the Hamiltonian including the spin using exact diagonalization method. We had investigated the dependence of the magnetization on temperature, magnetic field and confining potential. The energy of the electron had been displayed as function of magnetic field, Gaussian confinement potential height and quantum dot size. The comparisons show that our results are in very good agreement with reported works.

Chapter One

Introduction

1.1 Quantum Confinement and density of states

The presence of many atoms in a bulk material causes splitting of the electronic energy levels, giving continuous energy bands separated by a forbidden zone. The reduction in the number of atoms in a material results in the confinement of energy states as shown in fig (1)

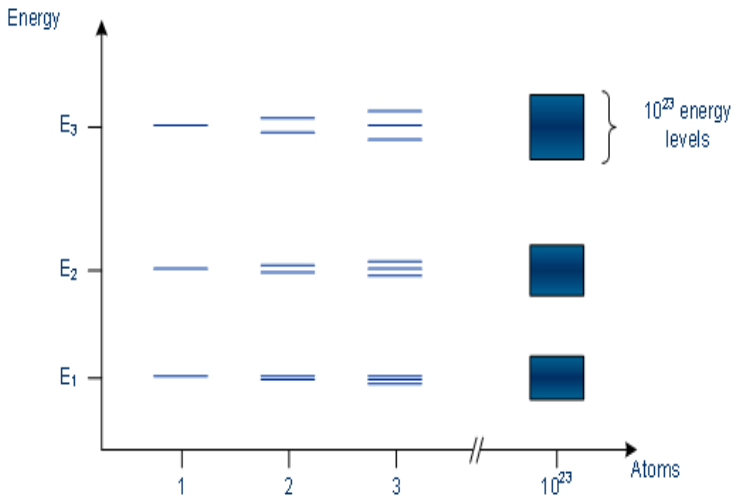

Fig (1.1) : The energy levels vs number of atoms in bulk material

Electron-hole pairs become spatially confined when the diameter of a particle approaches the De Broglie wavelength of electrons in the conduction band. As the material becomes small it shows quantum effects in their physical properties and their electronic and optical properties differ from those of bulk materials and the energy difference between energy bands is increased with decreasing particle size.

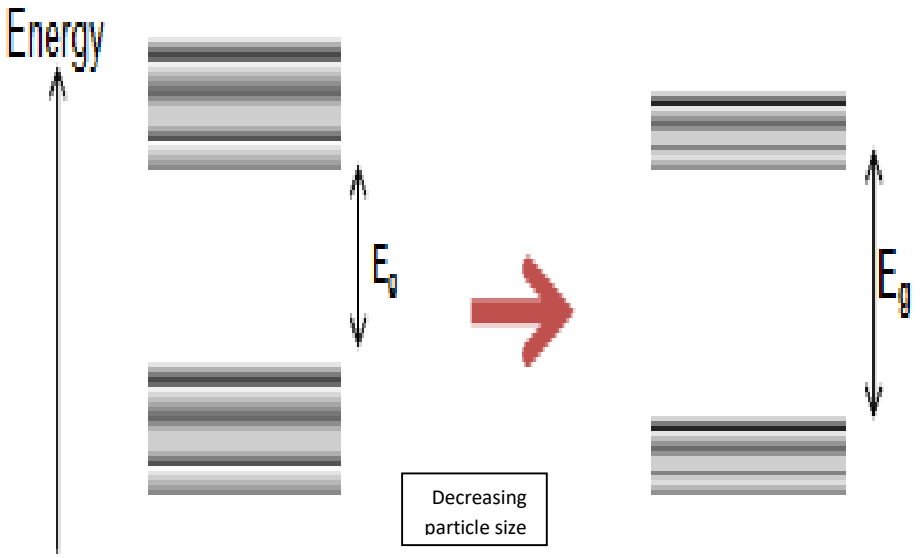

Fig (1.2) : Increasing the energy difference between energy bands with decreasing particle size

This is very similar to the famous particle-in-a-box and can be understood by the Heisenberg Uncertainty Principle which states that the more exactly one knows the position of a particle the more uncertainty in its momentum / (and vice versa). Therefore, the more spatially confined and

localized a particle becomes, the wider the range of its momentum/energy.

Quantum Confinement is the spatial confinement of electron in one or more dimensions within a material. No confinement: carriers act free in 3D as in bulk materials,1D confinement: carriers act free in 2D as in quantum wells ,2D confinement: carriers act free in 1D as in quantum wire and 3D confinement: carriers act free in 0D which means quantum dot (QD).

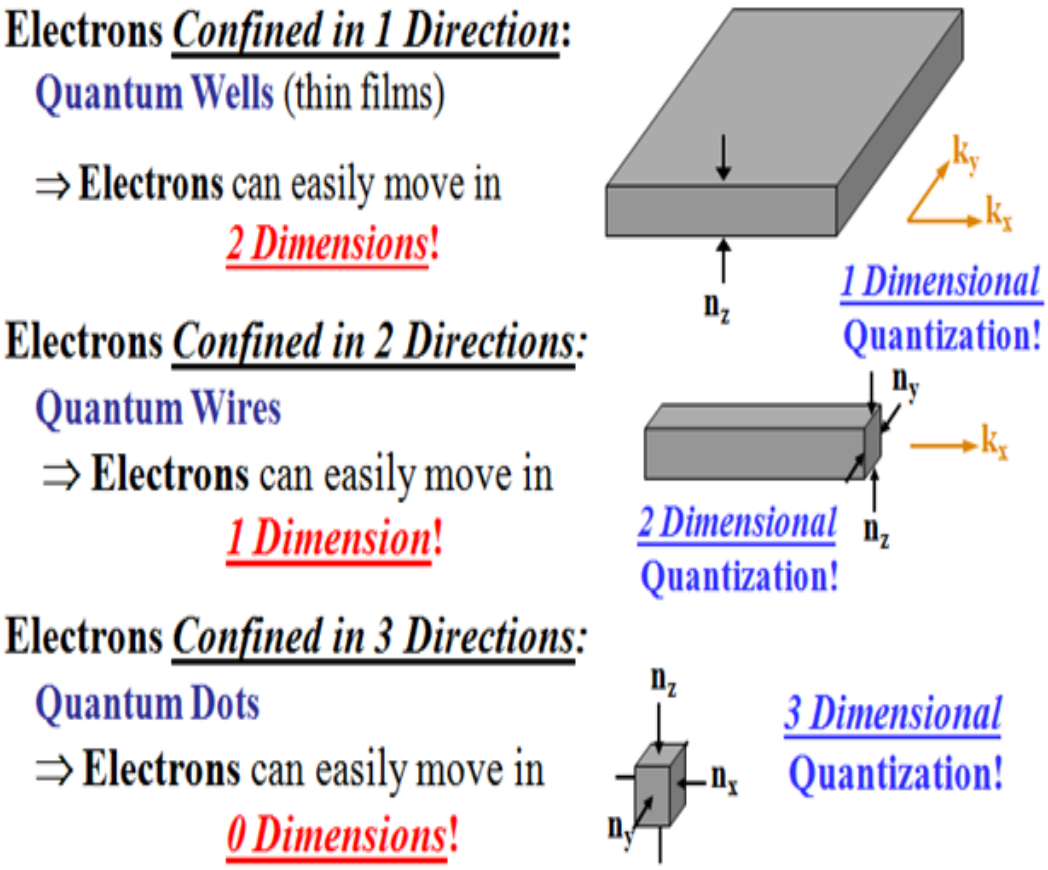

Fig(1.3) : Quantum Confinement in nanostructures

QDs are defined as nano - scale systems were carriers are confined in all three directions by using confining potential, so the energy spectra are completely discrete and quantized which leads to many unique optical and transport properties. QDs are usually regarded as semiconductors. Similar behavior is observed in few metals. Therefore, in some cases it may be acceptable to speak about metal quantum dots.

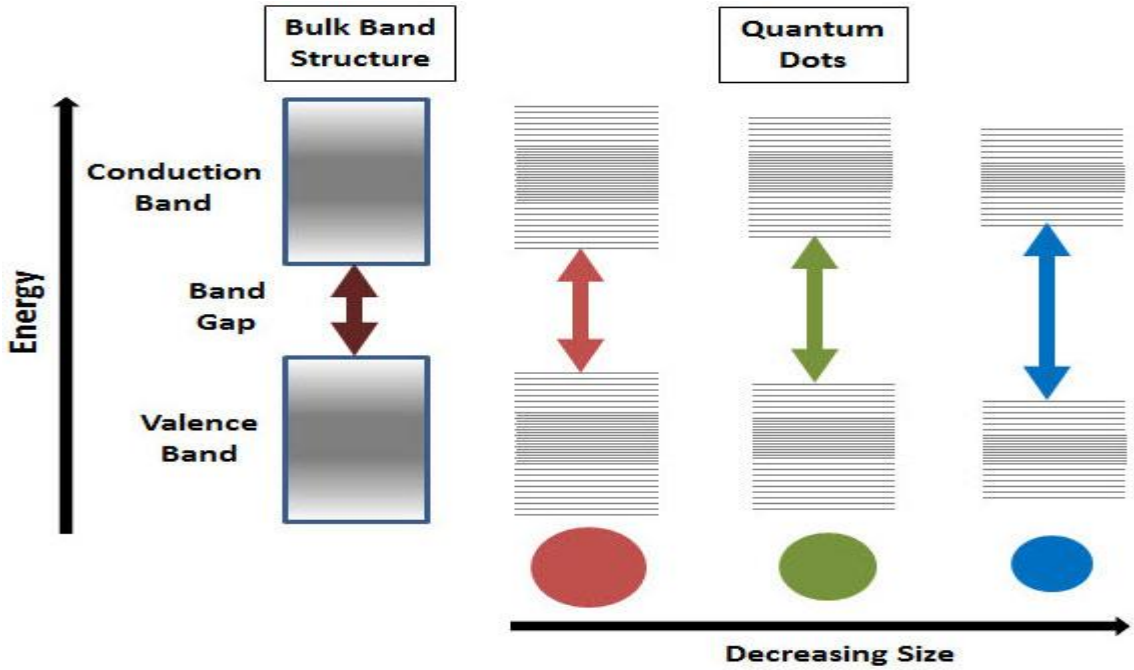

Fig(1.4) : Controlling the bandgap by quantum dots size

QDs bandgap can be controlled by its size. So we can engineer their optical and electrical properties. Smaller QDs have large bandgaps as shown in fig (4).

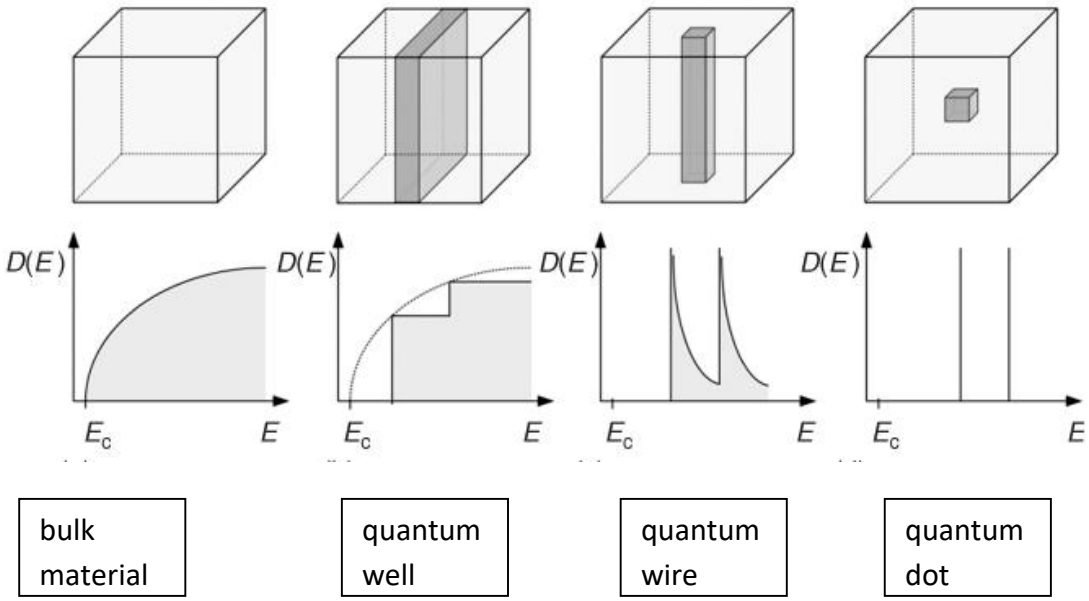

Fig(1.5) : Density of states for bulk materials, quantum well, quantum wire, and quantum dot

In fig (5) we sketch the density of states (number of states per unit energy) for bulk materials, quantum well, quantum wire, and quantum dot.

1.2 Fabrication methods and applications of QDs

QDs are fabricated by applying negative voltage to the metal electrodes on the surface of heterostructure, so the electron can be confined to one or zero dimension. This can be made by many methods like Electron-Beam Lithography and Molecular Beam Epitaxy (MBE).

Electron beam lithography (e-beam lithography) is a technique that uses an accelerated beam of electrons to pattern features down to sub-10 nm on substrates that have been coated with a positive or a negative electron beam sensitive resist as shown in fig (6).

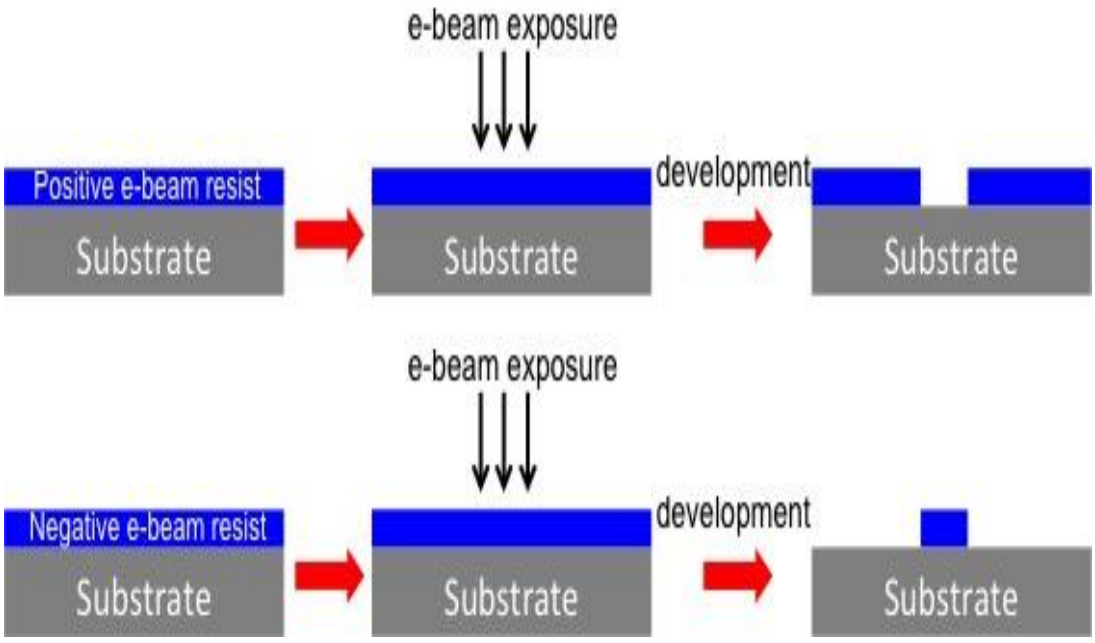

Fig(1.6) : Electron beam lithography technique

The other method is MBE which is a technique to grow crystalline thin films in ultrahigh vacuum with very precise control of thickness and formation.

Due to their unique properties, QDs have many applications, like QD LEDs, medical imaging, solar cells, single electron transistor and QD LASERs. Here I will speak briefly about some of these applications. For example, in the QD LEDs, the light emitting centers are cadmium selenide (CdSe) nanocrystals, or QDs so those LEDs can absorb and emit at any desired wavelength by controlling the size of the QD. QDs solar cells have the possibility to harvest light energy over a wide range of visible and IR- light and have almost 60% efficiency in electricity production.

1.3 Literature survey

Different authors had solved the QD Hamiltonian with parabolic potentials by using various methods [1-13]. The Gaussian potential has been proved to be the effective potential in many branches of physics. It has been solved approximately for a single particle problem by many authors [14,15]. The presence of Gaussian confinement potential type in a single electron quantum system makes the analytic solution of the Hamiltonian not attainable. Many methods, including perturbation and variation, were used to solve this problem. Boyacioglu and Chatterjee applied perturbation method to study the dia and paramagnetism and total susceptibility of GaAs QD with Gaussian confinement [16]. Boda and Chatterjee studied the transition energies and magnetic properties of a neutral donor complex in a

Gaussian GaAs QD [17]. Khordad examined the pressure effect on the optical properties of modified Gaussian QD [18]. Baser et.al. studied the hydrostatic pressure and temperature effects on the binding energy of the magnetoexcitons in cylindrical quantum well wire [19]. Gharaati and Khordad considered the modified Gaussian potential as a confinement one in spherical QD [20]. Al-Hayek and Sandouqa investigated the binding energy of donor impurity in QD with Gaussian confinement [21]. However, Rahmani et.al. computed the diamagnetic susceptibility of a confined donor in inhomogeneous QD [22]. Hong, et.al. studied the impurity related electronic properties in QD under electric and magnetic field using Gaussian potential as confinement potential with the help of variational calculation [23]. Anil Kumar has considered the ground state properties of two dimensional QD Helium in zero magnetic field and parabolic confinement potential by using diagonalization, perturbation and variational theory [24]. Also, Xie studied the linear and nonlinear optical properties of an off-center hydrogenic impurity in a spherical QD with the Gaussian potential using the matrix diagonalization method [25]. Very recently, Bzour searched in the effects of hydrostatics pressure and temperature on the properties of the GaAs single QD in an external magnetic field with the help of exact diagonalization technique [26]. Shaer looked for the heat capacity of two electrons QD in an external magnetic field by using variational method [27]. Very recently, Elsaid *etal* had used variational and exact diagonalization methods to study the electronic, thermodynamic and magnetic properties of a single and coupled QDs [28-35].

In this work, the exact diagonalization method has been used to solve the Hamiltonian and obtained the energy spectra of single electron quantum system in external magnetic field with presence of Gaussian confinement potential. In addition, the magnetization has been calculated by using the energy spectra which we obtained from solving the QD Hamiltonian as a necessary input data.

1.4 Research objectives

Our aims of this research are:

1-Solving the Hamiltonian by using exact diagonalization method to calculate the energy spectra of the system.

2- Calculating the magnetization of single electron QD system in the presence of an external magnetic field.

Chapter Two

Theory of single QD

2.1 QD Hamiltonian with Gaussian potential

The Hamiltonian of a single electron system in external magnetic field with presence of Gaussian confinement potential is given as,

$$\hat{H} = \frac{1}{2m*}(\vec{P} + \frac{e}{c}\vec{A})^2 + V(\rho) \quad (1)$$

Where $\vec{\rho}$ refers to the position vector of an electron, $\vec{P}$ the momentum operator , m*is the electron effective mass, $\vec{A}$ is the vector potential corresponding to the applied magnetic field $\vec{B}$ along z direction including the spin Zeeman term. The magnetic field given by $\vec{B}=\vec{\nabla}\times\vec{A}$ and V(ρ) is the confining potential which we take as Gaussian potential,

$$V(\rho) = -V_0 e^{-\rho^2/2R^2} \quad . \quad (2)$$

The Hamiltonian can be rewritten as,

$$\hat{H} = -\frac{\hbar^2}{2m^*}\vec{\nabla}^2{}_\rho + V(\rho) + \frac{1}{8}m^*\omega_c{}^2\rho^2 + \frac{1}{2}\hbar\omega_c(\hat{L}_z + g^*\hat{S}_z), \quad (3)$$

where $\hat{L}_z$ is the z component of the angular momentum of the electron, ω_c is the cyclotron frequency given by $\omega_c = eB/m^*$, B being the strength of the applied magnetic field , R is quantum dot radius,V_0 is the depth of the confining potential and g*is the effective Lande-g factor which equal -0.44 for GaAs.

2.2 Exact diagonalization method

The Gaussian potential term makes the analytical solution of this system not possible. We intend to solve the Hamiltonian by using the exact diagonalization method. The bases are Fock-Darwin states [36,37], given as, $|nm_z>$

Where $|nm_z> = \frac{\alpha}{\sqrt{\pi}} \left(\frac{n!}{(n+|m_z|)!}\right)^{\frac{1}{2}} (\alpha\rho)^{|m_z|} L_n^{|m_z|}(\alpha^2\rho^2) \; e^{\frac{-1}{2}\alpha^2\rho^2} e^{im_z\phi}\chi(\sigma)$ (4)

where $\alpha = \sqrt{m^* \omega/\hbar}$ (5)

n is the radial quantum number , m_z is the azimuthal angular momentum quantum number, $L_n^{|m_z|}$ is the associated Laguerre polynomial and $\chi(\sigma)$ is the eigenstate of the spin operator $\hat{S}_z$.

By rewriting the Hamiltonian as $\hat{H} = \hat{H}_0 + \hat{H}_1$

where,

$$\hat{H}_0 = -\frac{\hbar^2}{2m^*}\vec{\nabla}^2_\rho + \frac{1}{2}m^*\omega\rho^2 + \frac{1}{2}\hbar\omega_c(\hat{L}_z + g^*\hat{S}_z) \quad (6)$$

$$\hat{H}_1 = -\frac{1}{2}m^*\omega_0^2\rho^2 - V_0 e^{-\rho^2/2R^2} \quad (7)$$

Where ω^2 is the effective frequency,

with $\omega^2 = \omega_0^2 + \frac{1}{4}\omega_c^2$ (8)

We can write the matrix elements of the Hamiltonian in terms of these bases using eq. 4, as

$$<\acute{n}m_z|\ \widehat{H}|nm_z> = \langle \acute{n}m_z|\widehat{H}_0|nm_z\rangle + \langle \acute{n}m_z|\ \widehat{H}_1|nm_z\rangle$$

$$= (2n + |m_z| +1)\ \hbar\omega\ + \frac{1}{2}\hbar\omega_c\ (m_z + g^*S_z\ )$$

$$+ <\acute{n}m_z|\ -V_0 e^{-\rho^2/2R^2}|nm_z\rangle\ \ -$$

$$<\acute{n}m_z|\ \frac{1}{2}\ m^*\omega_0{}^2\ \rho^2\ |nm_z\rangle \qquad (9)$$

The first term represents the Harmonic oscillator case with well-known eigenenergy and eigenfunctions and the matrix element for the Gaussian confinement potential $<\acute{n}m_z|\ -V_0 e^{-\rho^2/2R^2}|nm_z\rangle$ was evaluated in a closed form by using the following Laguerre relation [38],

$$\int_0^\infty t^{\alpha-1}e^{-pt}L_m^\lambda(at)L_n^\beta(bt)dt\ =$$

$$\frac{\Gamma(\alpha)(\lambda+1)_m(\beta+1)_n p^{-\alpha}}{m!n!}\sum_{j=0}^{m}\frac{(-m)_j(\alpha)_j}{(\lambda+1)_j\ j!}\left(\frac{a}{p}\right)^j\sum_{k=0}^{n}\frac{(-n)_k(\alpha+j)_k}{(\beta+1)_k\ k!}\left(\frac{b}{p}\right)^k \qquad (10)$$

This closed form reduces significantly the computation time needed in the diagonalization process.

2.3 The magnetization:

We calculated the magnetization (M) of the confined electron in the QD by differentiating the average statistical energy partially with respect to the magnetic field as follows,

$$M= -\frac{\partial<E>}{\partial B} \qquad (11)$$

$$\text{Where } <E> = \sum_j \frac{E_j e^{-\frac{E_j}{K_B T}}}{\sum_j e^{-\frac{E_j}{K_B T}}} \qquad (12)$$

Chapter Three

Results and Discussion

In this chapter we will present our computed results for the energy spectra of a single electron presented in a magnetic field which are essential input data to calculate the average energy as a first step. Next, we compute the magnetization by using the energies which we obtained. Diagram and tables were used to illustrate the results. The results will be tested against reported ones.

3.1 QD energy Spectra

We first calculate the ground state energy of the QD for fixed potential height (V_0) and different QD radii, then we test our computed results with recent ones published by Boyacioglu and Chatterjee [39]. The results are listed in Table (3.1). The comparison clearly shows excellent agreement of both works as the QD radius increases. For example, at small radius R=10nm, the calculated energies show small variations (-19.1188 and -18.5236) for exact diagonalization and average field approximation, respectively. On the other hand, the energies become almost exact (-26.6895 and -26.5953) at large radius (R=19nm). In Fig (3.1) we plot ($E-V_0$) VS the QD radius (R) for the ground state with zero magnetic field(B=0) and with constant V_0. The figure shows the agreement between the energies of the exact (——) and average field approximation (…….) using Gaussian potential in both works. The accuracy increases as the QD radius becomes large. On the other hand, the

parabolic confinement potential model (------) shows a deviation from the Gaussian confinement type at small quantum dot radii. For large QD radius both models give close results.

We have shown in fig (3.2) the ground state and a few excited state energies of the Gaussian QD against B. The figure shows clearly the effect of the

Table (3.1): The ground state energy of a single electron GQD at B=0, and V_0=36.7 meV as function of R obtained from exact diagonalization method compared with Boyacioglu and Chatterjee (2012) work [39].

R(nm)	E-V_0(meV) our results	E-V_0(meV) Boyacioglu and Chatterjee (2012)
10	-19.1188	-18.5236
11	-20.4634	-20.0091
12	-21.6234	-21.2689
13	-22.633	-22.351
14	-23.5187	-23.2908
15	-24.3014	-24.1146
16	-24.9977	-24.8427
17	-25.621	-25.4909
18	-26.182	-26.0718
19	-26.6895	-26.5953

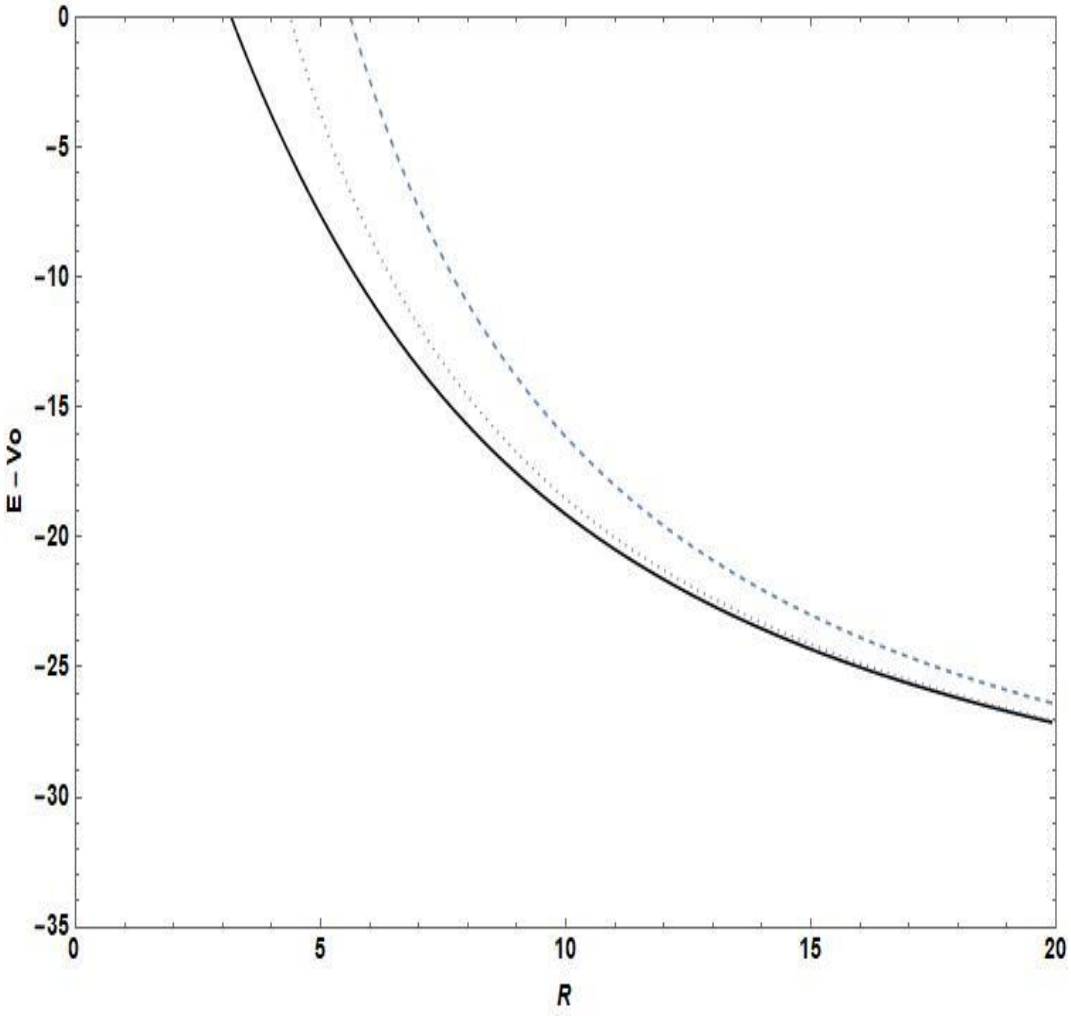

Fig (3.1): Ground state energy of a single electron Quantum dot as function of the potential range R at zero magnetic field B=0 and V_0=36.7meV. The dashed curve (-----) for PQD , the dotted curve(……) for GQD which solved by Boyacioglu and Chatterjee[39] by average field approximation and the solid curve(——)for GQD which we calculated by exact diagonalization method**.**

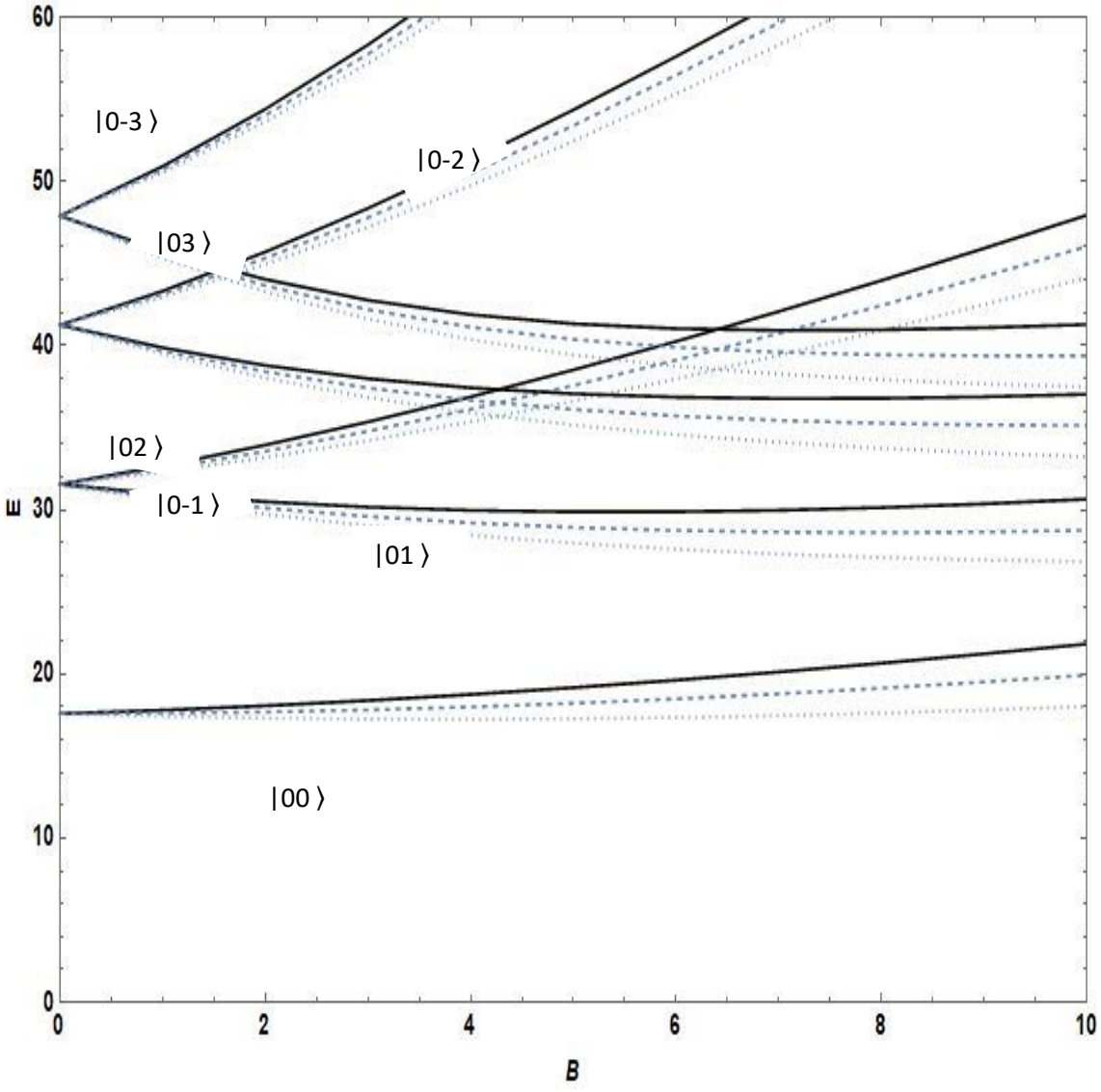

Fig (3.2): computed results of one electron GQD against magnetic field at V_0 = 36.7 meV and R=10 nm. The dashed curve(-----) for S=0 ,doted curve(…….) for S=1/2 and the solid curve(——) for S=−1/2.

Next, we found the average thermal energy of the ground state of the QD as in fig (3.3). This figure describes the average thermal energy against the magnetic field for PQD and GQD both calculated by Chatterjee approach and exact diagonalization method at different temperatures, taking into account the effect of the electron spin term. It is clear from the figure that,

the results produced by average field approximation method show discrepancy compared with the present results computed by exact diagonalization method.

By focusing on the results obtained by exact diagonalization method (——) we can see that at 0.005 K the energy decreases as the magnetic field increases , this behavior continues up to $B \approx 4$ T, then the energy starts increasing as the magnetic field increases .

As the temperature increases, from 0.005K to 10 and 30 K, the ground state energy curve of the QD shows a great enhancement. This behavior is due to the significant increment in the thermal and the confinement energy contributions. The same behavior is also seen for PQD and GQD shown by Chatterjee et.al.[36]. The effect of the spin on the statistical ground state energy is very clear by comparing the results in Tables (3.2) and (3.3) for zero and non-zero spin case, respectively. The spin reduces the ground state energy due to its negative energy contribution ($-0.44 \frac{\hbar\omega_c \, Sz}{2}$). For example, at B=10T and T=20K, the ground state energies of the QD are 19.9824 meV and 18.4584 meV, as Tables (3.2) and (3.3) show, respectively.

To emphasize the important role of the spin on the QD ground state energy, we have plotted in Fig (3.4), separately, the average statistical energy <E> against the magnetic field strength B at low temperature, T=5mK. The figure again shows the significant effect of the spin, particularly at high magnetic field.

Figures (3.5,3.6 and3.7) show the effect of the potential depth V_0 on the behavior of the curve of the statistical energy <E> against the strength of B

at different temperatures. The figures show clearly the great change in the behaviors of the energy curves as we increase the confining Gaussian potential from: 36.7meV to 150 meV.

The Gaussian potential term ($-V_0 e^{-\rho^2/2R^2}$) increases greatly the total energy of the ground state due to its large Gaussian energy confinement. For example, at T=30K the statistical energies are:19meV ,31.1meV and 38.6meV at B=10T for V_0=36.7meV, 100meV, 150meV, respectively.

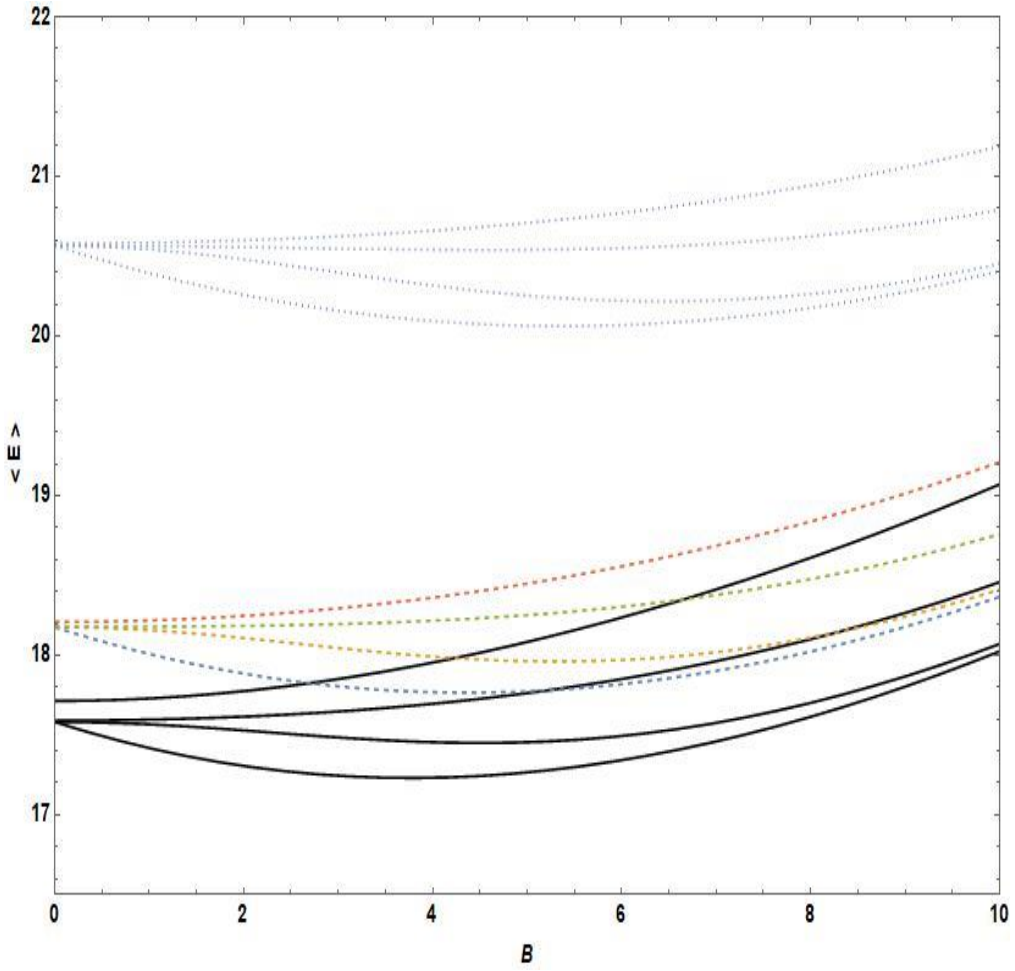

Fig(3.3): The average thermal energy versus the strength of the magnetic field for PQD dotted curve(……..) and for GQD for both average field approximation dashed curve(-----) and exact diagonalization method solid curve(——) at T = 5 mk , 10, 20, and 30 K from bottom to top.

Table (3.2): The average thermal energy of GQD obtained from exact diagonalization method as function of B at V_0=36.7 meV, R=10nm, g*=0 (no spin) for T = 5 mk, 1, 10, and 20K

B(T)	<E>(meV) at T=.005K	<E>(meV) at T=1K	<E>(meV) at T=10K	<E>(meV) at T=20K
0	17.5826	17.5826	17.5826	17.5912
1	17.6088	17.6089	17.6089	17.6181
2	17.6871	17.6871	17.6871	17.6981
3	17.816	17.8161	17.8161	17.83
4	17.9936	17.9937	17.9937	18.0115
5	18.2173	18.2174	18.2174	18.2399
6	18.4844	18.4844	18.4845	18.5123
7	18.7917	18.7918	18.7919	18.8257
8	19.1365	19.1365	19.13.67	19.1771
9	19.5157	19.5158	19.516	19.5636
10	19.9268	19.9269	19.9272	19.9824

Table (3.3): The average thermal energy of GQD obtained from exact diagonalization method as function of B at V_0=36.7 meV, R=10nm, g*=−0.44(with spin) for T = 5 mk , 1, 10, and 20K .

B(T)	<E>(meV) at T=.005K	<E>(meV) at T=1K	<E>(meV) at T=10K	<E>(meV) at T=20K
0	17.5826	17.5826	17.5826	17.5912
1	17.4186	17.4232	17.5676	17.5972
2	17.3067	17.3068	17.5295	17.6156
3	17.2454	17.2455	17.4856	17.6479
4	17.2328	17.2329	17.4556	17.6962
5	17.2663	17.2664	17.4554	17.7631
6	17.3432	17.3432	17.4946	17.8513
7	17.4603	17.4604	17.5768	17.9633
8	17.6148	17.6149	17.702	18.1009
9	17.8039	17.804	17.8678	18.1657
10	18.0248	18.0249	18.0709	18.4584

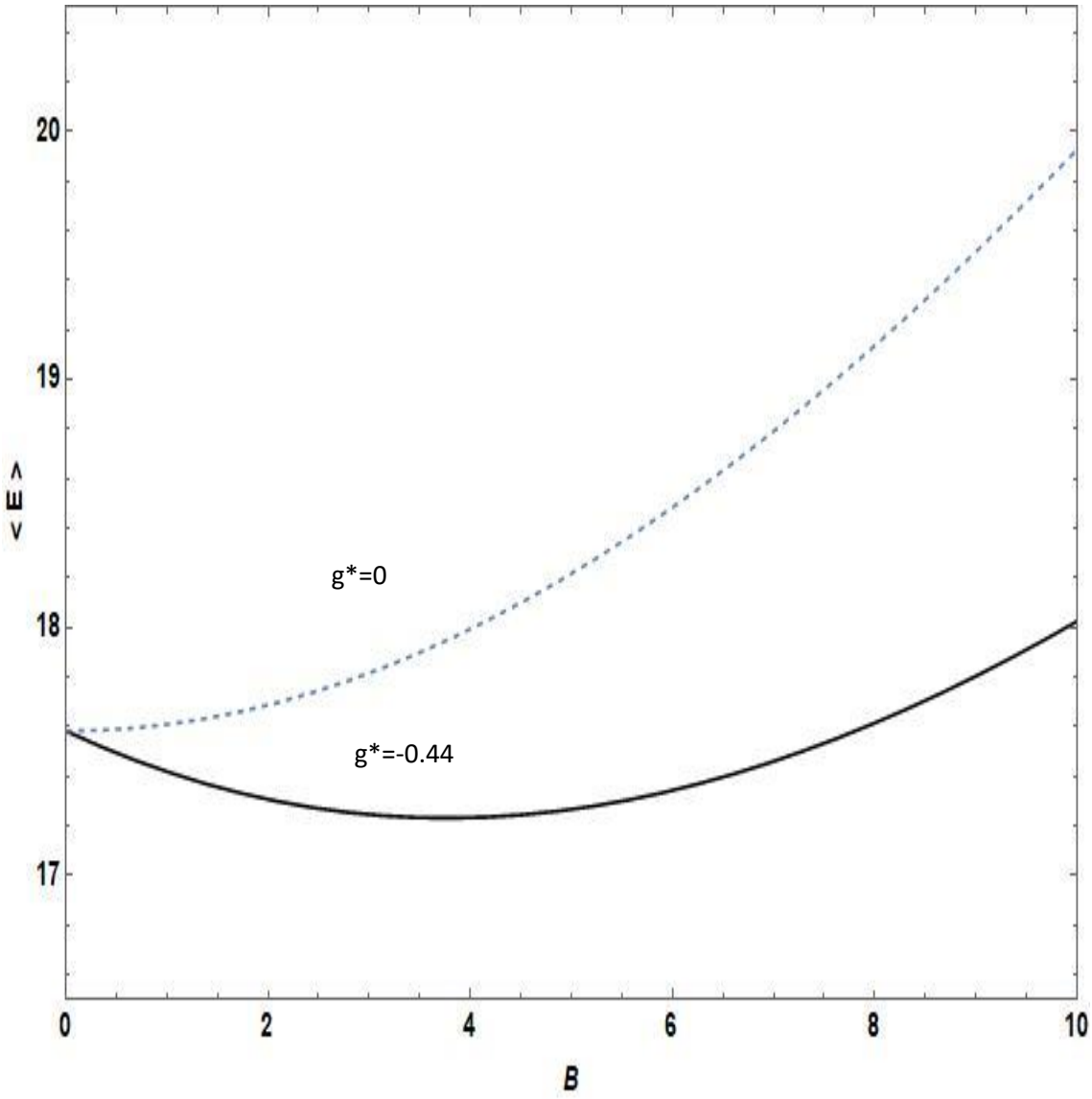

Fig(3.4): The average thermal energy against the strength of the magnetic field at T=5mK,V_0 =36.7 meV ,R=10nm and g*=0 and −0.44.

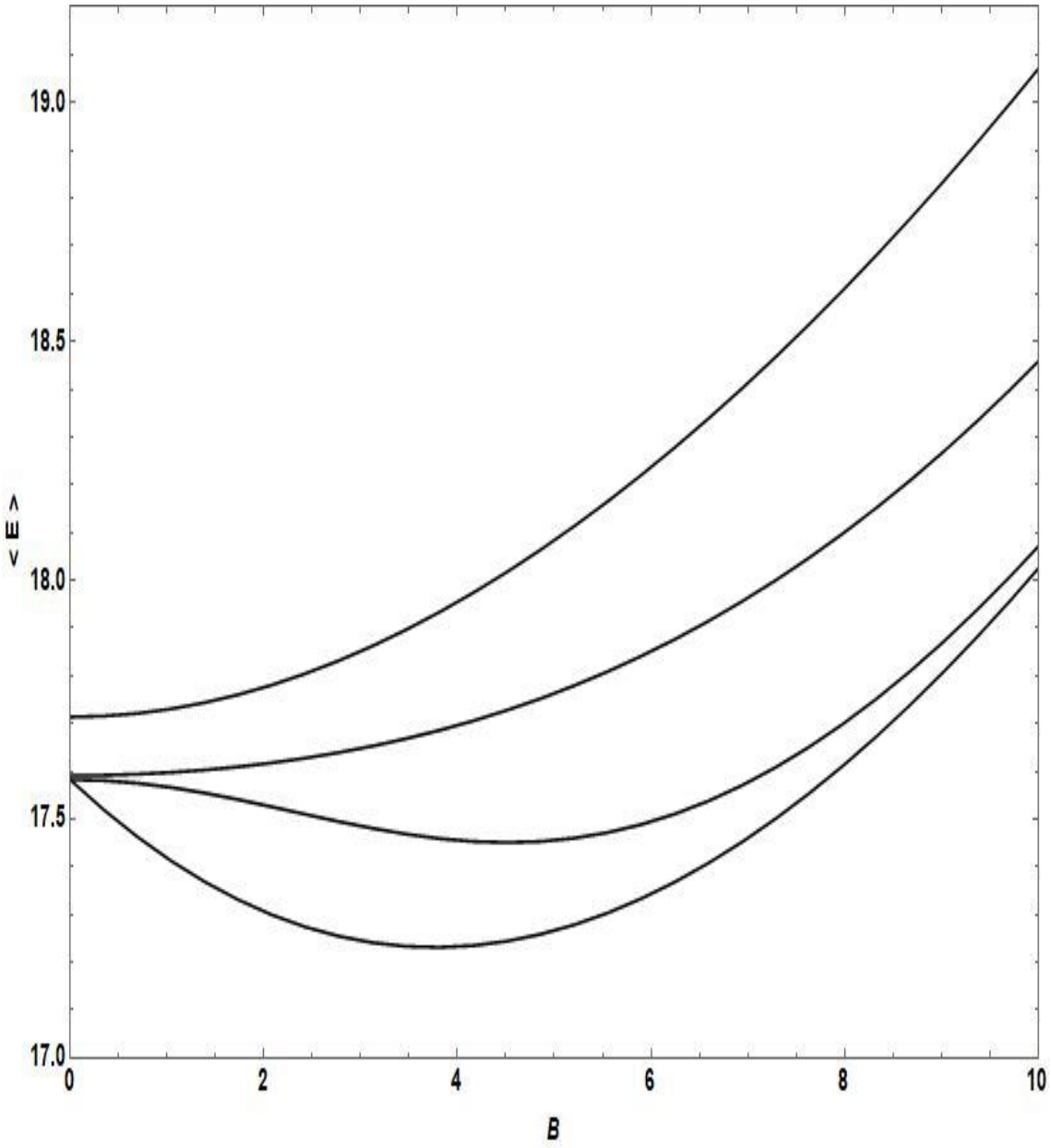

Fig(3.5): The average thermal energy<E> against the strength of the magnetic field B at V_0 =36.7 meV ,R=10nm, g*= −0.44 and T = 5 mk , 10, 20, and 30 K from bottom to top.

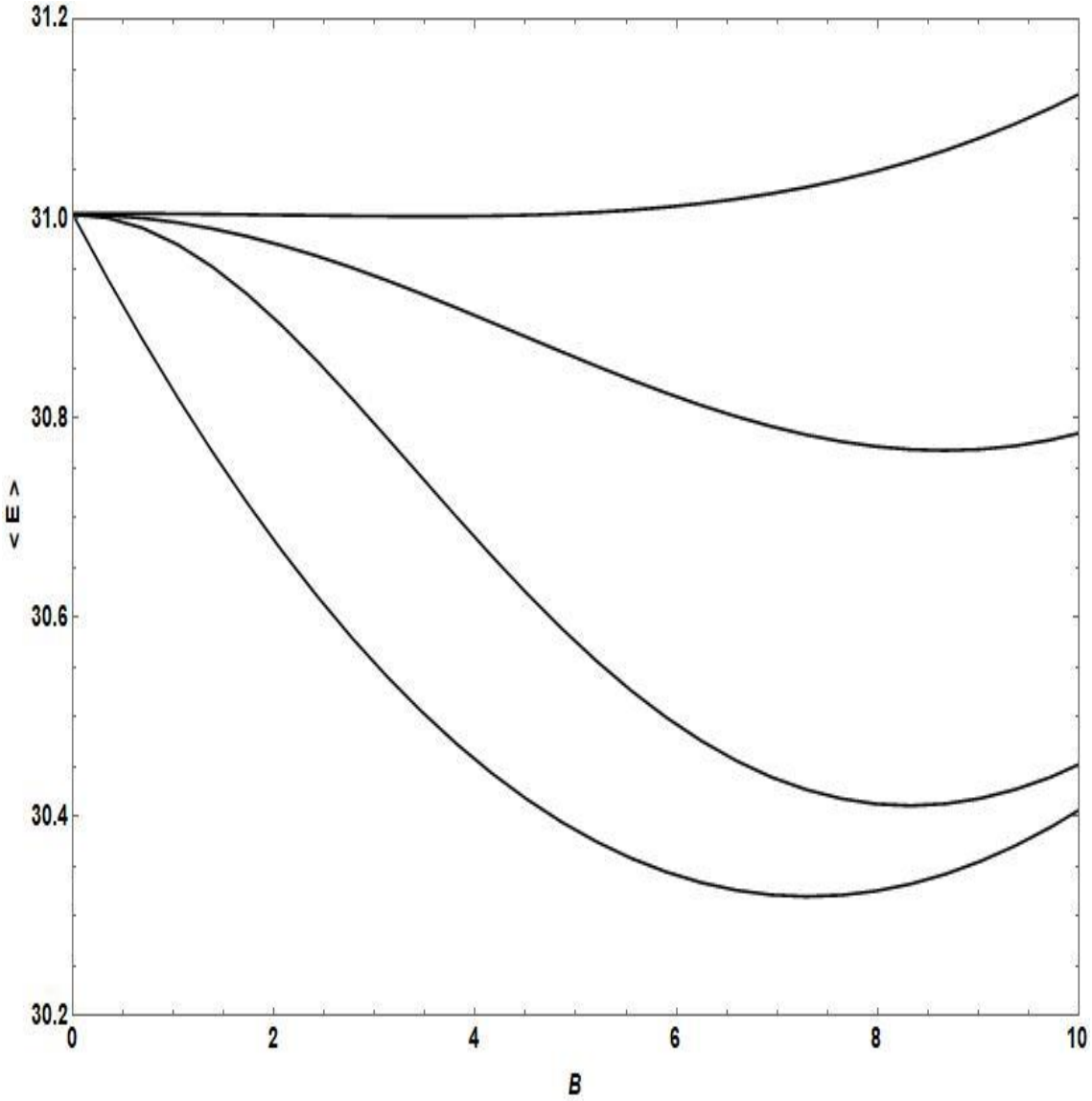

Fig(3.6): The average thermal energy<E> against the strength of the magnetic field B at V_0 =100 meV ,R=10nm, g*= −0.44 and T = 5 mk, 10, 20, and 30 K from bottom to top.

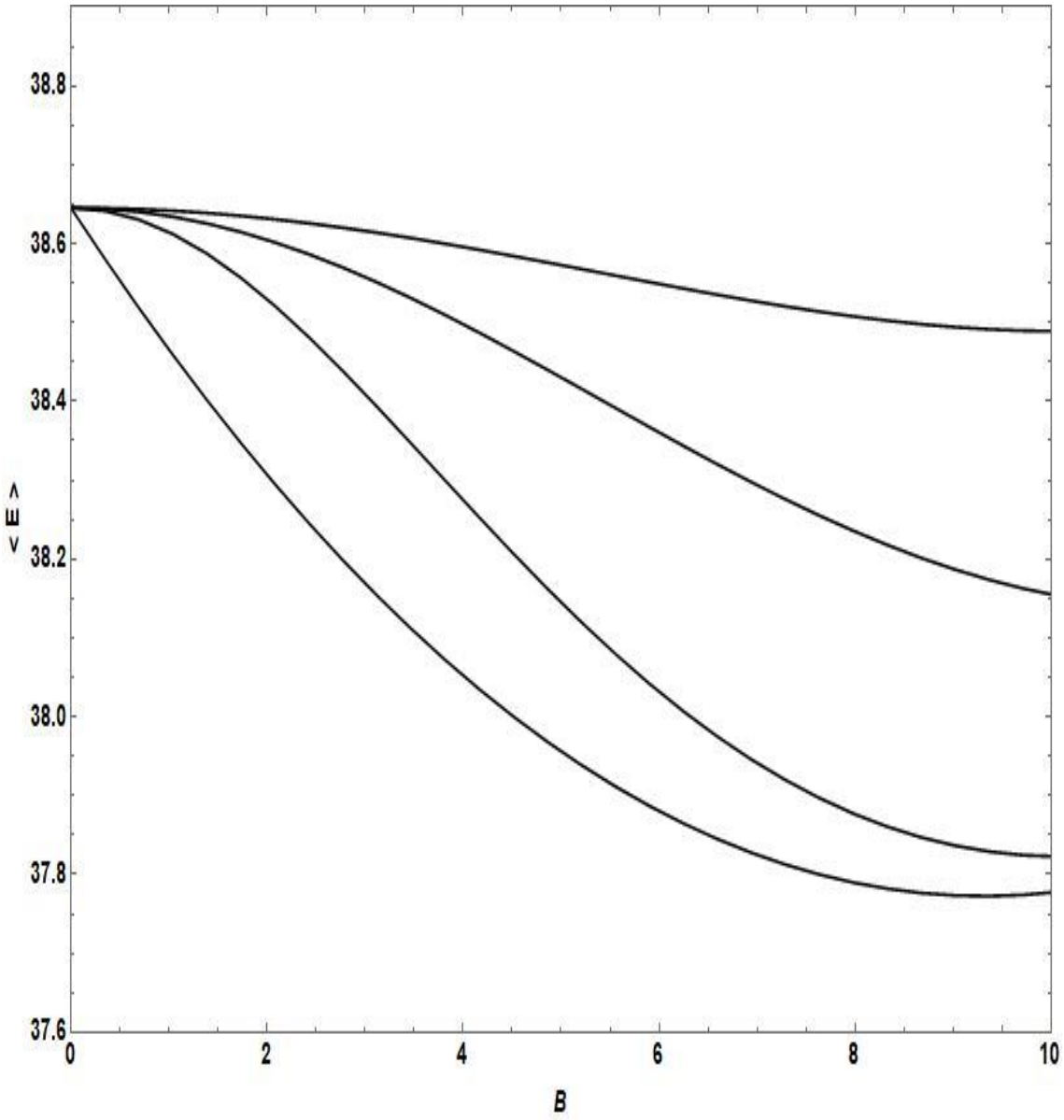

Fig(3.7): The average thermal energy<E> against the strength of the magnetic field B at V_0 =150 meV ,R=10nm, g*= −0.44 and T = 5 mk , 10, 20, and 30 K from bottom to top.

To test the convergence issue of our computed results, we plotted in fig (3.8) the ground state energy (E) with constant B=2 T, R=10 nm and V_0=36.7 meV versus the number of bases(n). The figure shows obviously great numerical stability in our computed work. We found that the number of bases n=10 is an excellent choice which gives high accurate energy results.

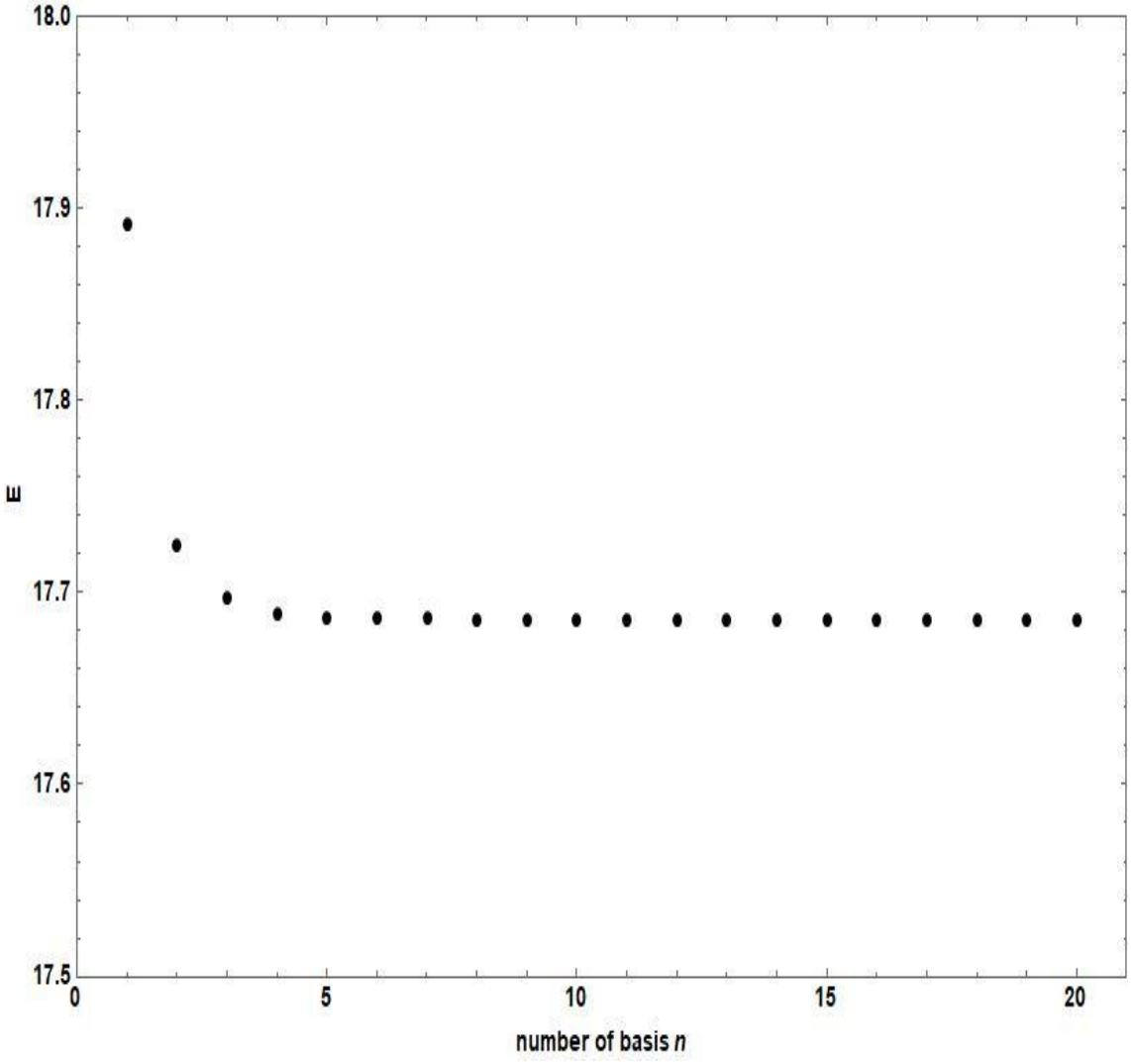

Fig (3.8): The computed energy of a single electron QD against the number of basis n at m=0, B=2T, V_0=36.7 meV and R=10 nm.

3.2 Magnetization

In this section we will present our computed results for the magnetization (M) of a single electron QD confined by a Gaussian potential. M was calculated by using the computed ground state energy of a confined electron in a QD as essential input data. Fig (3.9) represents M of a ground state against B for both PQD and GQD. In this graph the solid curve (—)

represents our computed results with Gaussian confinement using exact diagonalization method. The computed results were compared with the corresponding ones obtained by Chatterjee et.al [39] using average field approach with Gaussian confinement (-----), and with the PQD results (…….).It is clear from the figure that |M| increases when B increases. This behavior of the magnetization is in qualitative agreement with the results reported by Chatterjee etal [39].

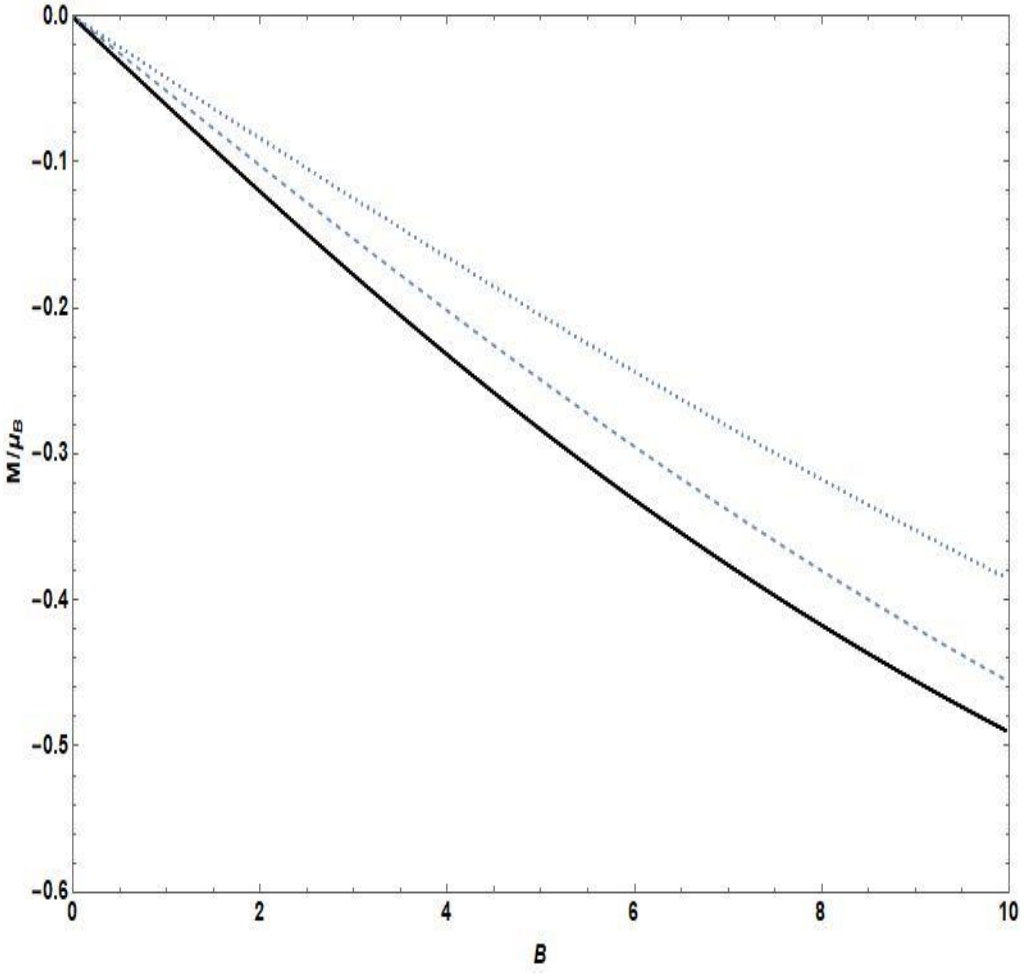

Fig(3.9): The magnetization per effective Bohr magneton$\frac{\boldsymbol{M}}{\mu_{\boldsymbol{B}}^{*}}$ against the strength of the magnetic field B at m=0, V_0=36.7 meV, T=0 and R=10 nm for PQD dotted curve(……..) and GQD for Chatterjee approach dashed curve(------) and exact diagonalization method our work solid curve(——) .

In fig (3.10), we present the dependence of M on B for fixed values of the confinement depth (V_0) and R calculated at different temperatures. For low temperature values (T=0.005K,1K,5K and 10k), M increases as B increases, reaching a peak value, then it starts decreasing. The effect of the temperatures on the magnetization curve is very significant. As the temperature increases the peak value in the magnetization curve decreases and becomes flat for fixed value V_0 and R. For high temperatures values (T=20K and 30K) the thermal energy ($E_{th}=K_BT$) becomes very significant and in this case it affects greatly the average energy behavior of the system as shown in figures (3.3). This leads to a linear decrease in the magnetization curve against the magnetic field. In addition, the effect of the depth of the confining potential (V_0) was also studied by taking different V_0 values, for example: (V_0=100mev) in fig (3.11) and (V_0=150mev) as in fig (3.12).

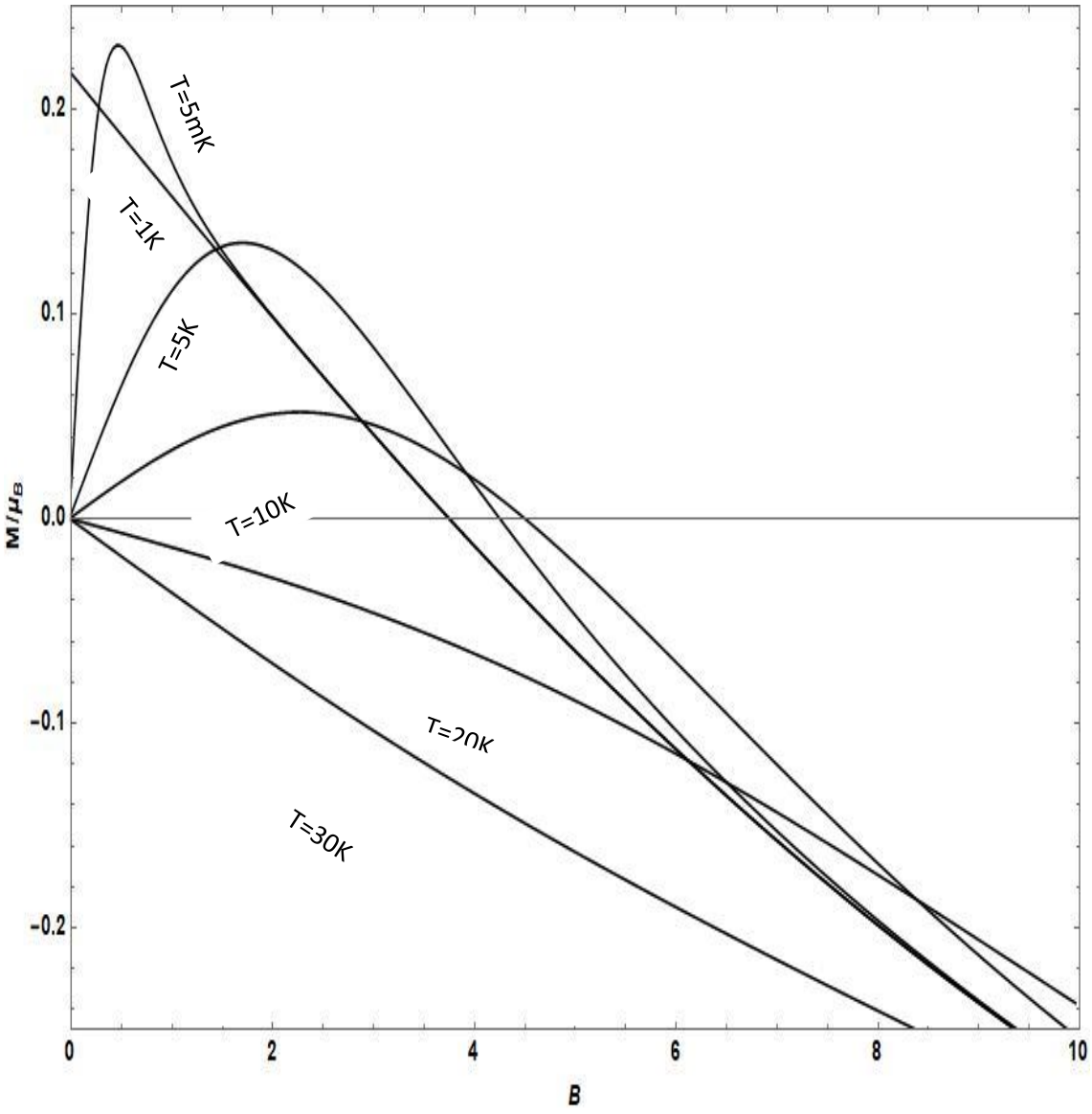

Fig(3.10): The magnetization per effective Bohr magneton$\frac{M}{\mu_B^*}$ against the strength of the magnetic field B at V0=36.7meV , R=10 nm and T=0.005 , 1,5,10,20 and 30K .

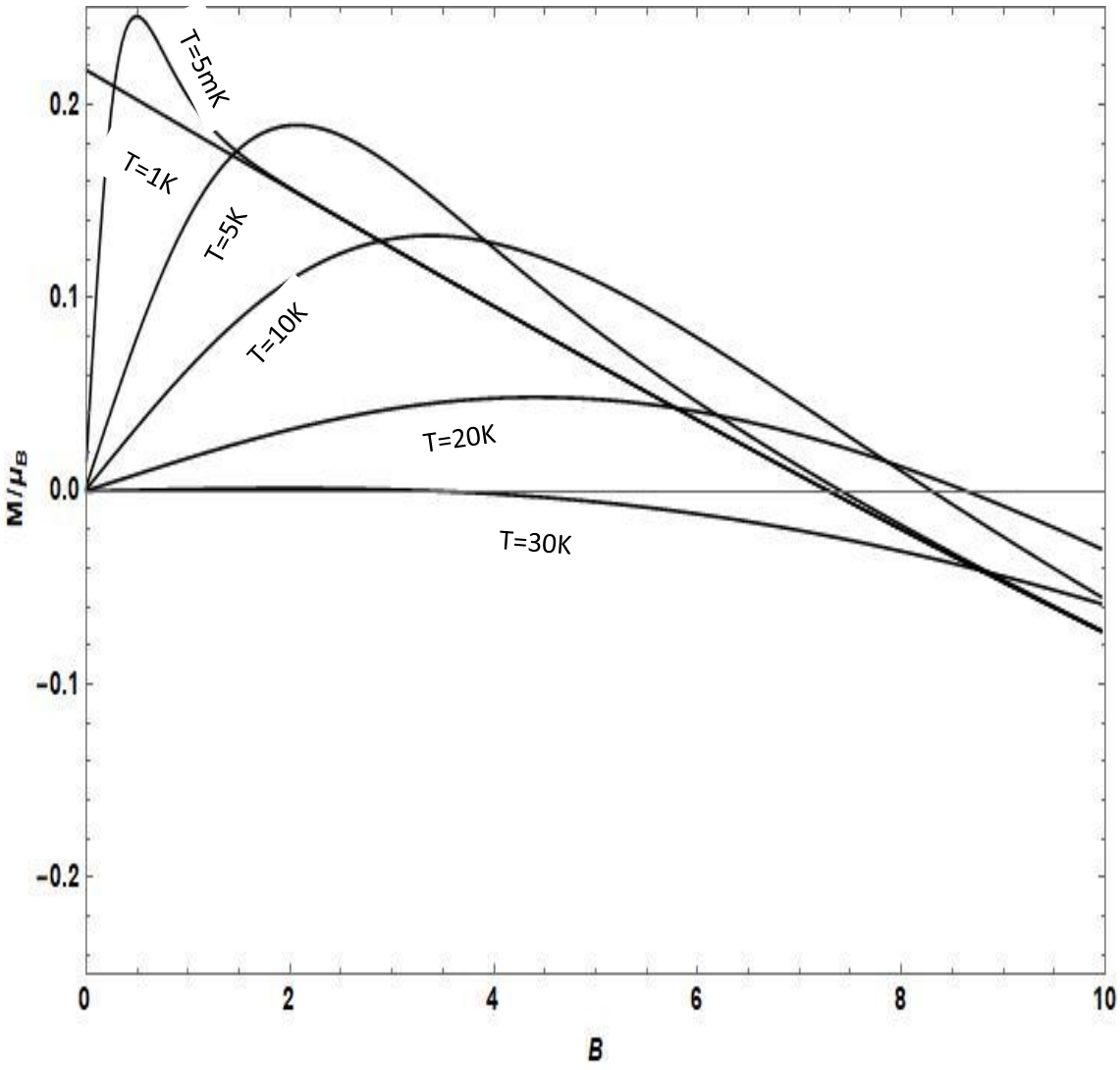

Fig (3.11): The magnetization per effective Bohr magneton$\frac{M}{\mu_B^*}$ against the strength of the magnetic field B at V_0=100meV , R=10 nm and T=0.005 , 1,5,10,20 and 30K.

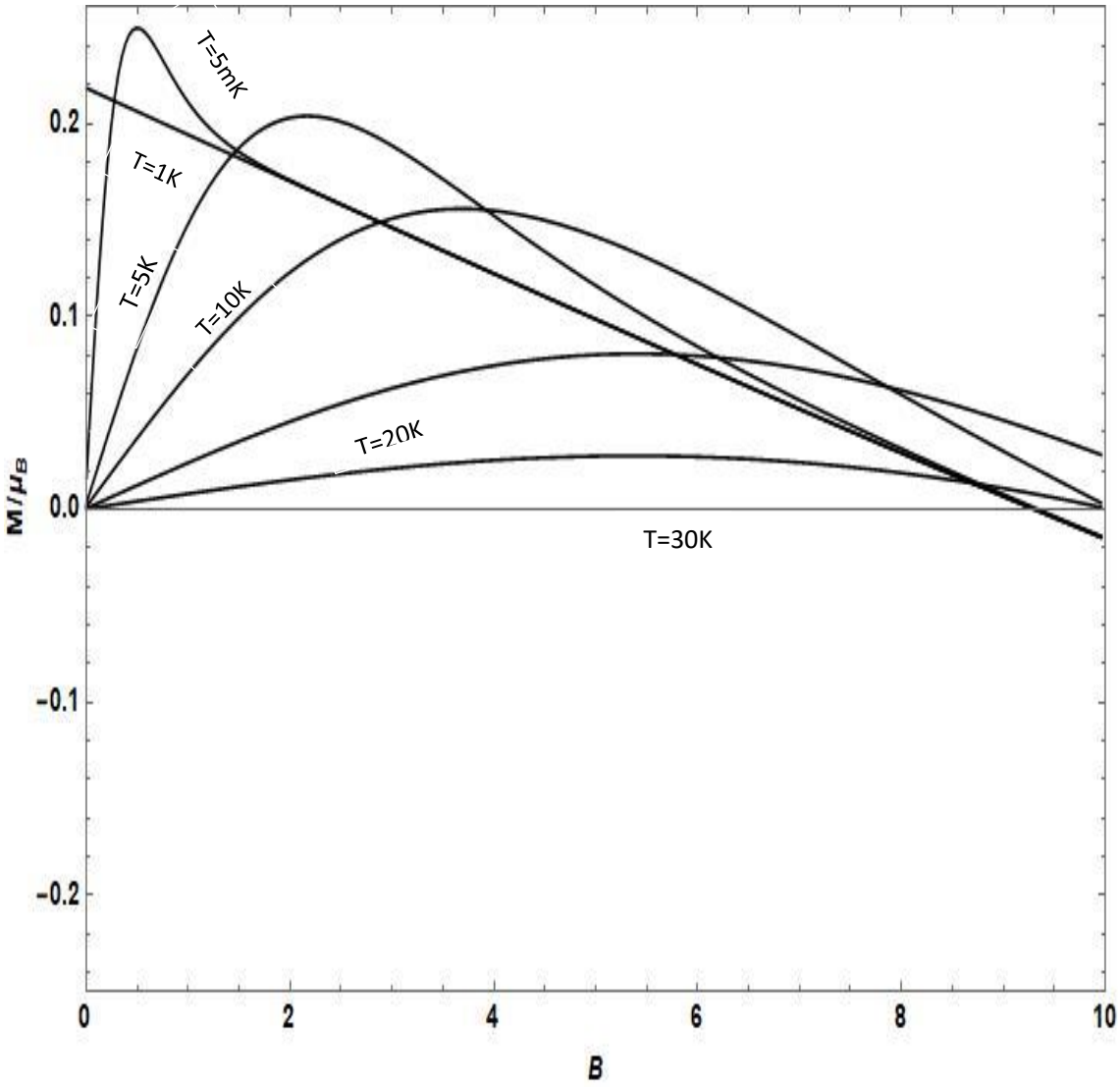

Fig(3.12): The magnetization per effective Bohr magneton$\frac{M}{\mu_B^*}$ against the strength of the magnetic field B at V_0=150meV , R=10 nm and T=0.005 , 1,5,10,20 and 30K .

Table (3.4): The peak values of the magnetization (M) against the magnetic field strength(B) for V_0 =36.7meV, R=10nm quantum dot and T=0.005,1,5,10,20 and30K.

$\frac{M}{\mu_B^*}$	B(T)	T(K)
0.21757	0	0.005
0.23125	0.4511	1
0.13478	1.7003	5
0.052	2.2555	10
No peak	////	20
No peak	////	30

Table (3.5): The peak values of the magnetization (M) against the magnetic field strength(B) for V_0 =100meV, R=10nm quantum dot and T=0.005,1,5,10,20 and30K.

$\frac{M}{\mu_B^*}$	B(T)	T(K)
0.21808	0	0.005
0.24597	0.4858	1
0.18959	2.082	5
0.13239	3.3659	10
0.04872	4.4069	20
0.00153	2.0126	30

Table (3.6): The peak values of the magnetization (M) against the magnetic field strength(B) for V_0 =150meV, R=10nm quantum dot and T=0.005,1,5,10,20 and30K.

$\frac{M}{\mu_B^*}$	B(T)	T(K)
0.2182	0	0.005
0.24933	0.4858	1
0.20376	2.1514	5
0.155662	3.6782	10
0.08049	5.3785	20
0.02758	5.3785	30

By looking at the three figures (3.10,3.11 and 3.12), we can notice the effect of changing the depth of the confining potential (V_0) on the behavior of magnetization curve at different temperatures. New peaks appeared at higher temperatures(20and30K) when the potential depth(V_0) increased. The peaks shifted to the right, towards a higher magnetic field strength and their values have become larger as shown in Tables: (3.4,3.5, and3.6). These peaks can be attributed to the effect of the potential depth (V_0) on the statistical energy behavior as shown in figures: (3.5,3.6 and 3.7).

Chapter Four

Conclusion and Future Work

Exact diagonalization method has been used to solve the QD Hamiltonian and to calculate the energy and the magnetization of a single GaAs quantum dot with Gaussian confinement as function of the magnetic field strength (B), QD radius(R) and temperature(T). In this work, we have shown the dependence of the energy on the QD radius(R) as a first step. Next, we have also calculated the statistical energy <E>, taking into account the presence of the spin (S). The QD-energy results are displayed against the physical parameter of the QD: the magnetic field strength (B), QD radius (R), the temperature (T) and the potential depth(V_0), We also discussed the effect of the spin (S) on the statistical energy behavior. In addition, we calculated the magnetization (M) of the ground state energy as function of the magnetic field strength (B) at constant(R) and (V_0). The obtained results are compared with the recent published works. We calculated the magnetization (M) as function of the magnetic field strength (B) at different values of the temperature (T), potential depth(V_0) and QD radius (R). The computed results allowed us to study the effect the potential depth(V_0) and the temperature(T) on the behavior of the peaks in the magnetization curves.

We intend to carry more research studies on the magnetic susceptibility χ and heat capacity (C_v) of this QD-system. under a uniform magnetic field, in the future.

Appendix: **The exact diagonalization method**

In this appendix we give the main essential steps which lead to the diagonalization of the Hamiltonian, $\hat{H}$.

By considering the eigenvalue equation as,

$$\hat{H}|\psi> = E|\psi> \qquad (A.1)$$

Where

$$|\psi> = \sum_n \varphi_{n>} \qquad (A.2)$$

Then by multiplying equation $(A.1)$ by bra as $<\varphi_m|$ for each side and notice that $\sum_n <\varphi_m|H|\varphi_n> = \sum_n H_{mn}$

The equation becomes,

$$\sum_n H_{mn} = E_n \sum_n <\varphi_m|\varphi_n> = E_n \delta_{mn} \qquad (A.3)$$

Where the basis are orthonormalized as shown,

$$\sum_n \langle\varphi_m|\varphi_n\rangle = \delta_{mn} \qquad (A.4)$$

$$<E_n> = <\varphi_m|H|\varphi_n> \qquad (A.5)$$

The Dirac matrix notation form can be written in integration form as,

$$E_n = \int_{-\infty}^{\infty} \psi^* H \psi \rho \, d\rho \, d\varphi \qquad (A.6)$$

Equation A.1 takes the following matrix form,

$$\sum_n [H_{mn} - E_n \delta_{mn}] = 0 \qquad (A.7)$$

The eigenvalues and eigenstates of A.7 can be obtained from the condition,

$$Det[H_{mn} - E_n \delta_{mn}] = 0 \qquad (A.8)$$

References

[1] C. Ciftja, ***Phys.* Scr. 72** ,058302 (2013).

[2] M. Wagner, M.U. Merkt, A.V. Chaplik, ***Phys.* Rev. B 45**, 1951 (1992).

[3] M. Taut, J. Phys. A: ***Math.* Gen. 27**,1045 (1994).

[4] O. Ciftja, A.A. Kumar, ***Phys***. **Rev. B 70**, 205326 (2004).

[5] O. Ciftja, M. Golam Faruk, ***Phys*. Rev. B 72**, 205334 (2005).

[6] B.S. Kandemir, ***Phys*. Rev. B 72**, 165350 (2005).

[7] B.S. Kandemir, J. ***Math*. Phys. 46**, 032110 (2005).

[8] M. Elsaid, ***Phys*. Rev. B 46,** 13026 (2000).

[9] M. Elsaid, ***Superlattices Microstruct.* 23**, 1237 (1998).

[10] W. Dybalski, P. Hawrylak, ***Phys*. Rev. B 72**, 205432 (2005).

[11] N.T.T. Nguyen, S. Das Sarma, ***Phys*. Rev. B 83**, 235322 (2011).

[12] P.A. Maksym, T. Chakraborty, ***Phys*. Rev. Lett. 65**, 108 (1990).

[13] M. Helle, A. Harju, R.M. Nieminen, ***Phys*. Rev. B 72**, 205329 (2005).

[14] N. Bessis, G.Bessis,B.Joulakian, J. ***Phys*. A 15,** 3679 (1982).

[15] C.S.Lai , J. ***Phys*. A 16,** L181 (1983).

[16] Bahadir Boyacioglu and Ashok Chatterjee, ***Physica* E 44**, 1826 (2012).

[17] Ashok Chatterjee, ***Superlattices Microstruct.* 97**, 268 (2016).

[18] R. Khordad , ***Physica* B 4077**, 1128 (2012).

[19] P. Baser, H.Dkaki , I.Demir and S.Elagoz , ***Superlattices Microstruct.* 63**, 100 (2013).

[20] A.Gharaati and R.Khordad , ***Superlattices Microstruct***. **48**, 276 (2010).

[21] I.Al-Hayek, A.S.Sandouqa, ***Superlattices Microstruct***. **85**, 216 (2015).

[22] K. Rahmani, I.Zorkani , and A.Jorio **,** ***Phys*. Scr. 83**, 035701 (2011).

[23] Zhang Hong, Zhai Li-Xue, Wang Xue, Zhang chun-Yuan and Liu Jian-Jun , Chin, ***Phys* B 20**, 037301 (2011).

[24] A. Anil Kumar , ***Phys*. Rev. 70,** 205326 (2004).

[25] Wenfang Xie , **Superlattices Microstruct. 48**, 239 (2010).

[26] F. Bzour, **M.Sc** thesis, An-Najah National University (2016).

[27] A.Shaer, **M.Sc** thesis, An-Najah National University (2015).

[28] E. Hjaz, M.K. Elsaid, M. Elhasan, J. Comput. **Theor.Nanosci**. 14 ,1700 (2017).

[29] F. Bzour, M.K. Elsaid, A . Shaer, **Applied Physics Research**. 9,77 (2017).

[30] M. Elsaid, E. Hijaz, Acta ***Phys.*** Pol. A 131,1491 (2017).

[31] M. Elsaid, E. Hjaz, A. Shaer, Int. J. Nano. ***Dimens*. 8,1** (2017).

[32] A. Shaer, M. Elsaid, M. Elhasan, Turk. J. ***Phys*. 40,209** (2016).

[33] A. Shaer, M.K. Elsaid, M. Elhasan, Chin. J. ***Phys*****. 54**, 391 (2016).

[34] A .Shaer, M.K. Elsaid, M. Elhasan, Jord. J**.** ***Phys*****. 9**, 87 (2016).

[35] A. Shaer, M.K. Elsaid, M. Elhasan, J. ***Phys*****. Sci.** Appl. 6, 39 (2016).

[36] Boyacioglu, Chatterjee , ***Physica*** **E 44,** 1826 (2012).

[37] De Groote, J.J.S, Hornos, J.E.M, Chaplik, A.V. ***Phys*****. Rev. B 46**, 12773 (1992).

[38] Nguyen, N .T.T,Das Sarma, S. ***Phys*****. Rev. B 83**, 235322 (2012).

[39] Boyacioglu, Chatterjee, Int. J. ***Mod Phys*****. B,** 1250018 (2012).

جامعة النجاح الوطنية
كلية الدراسات العليا

التمغنط لنقطة كمية منفردة من زرنخيد الغاليوم GaAs المحصورة بجهد جاوس

إعداد
محمود ماجد محمود علي

إشراف
أ.د. محمد السعيد

قدمت هذه الأطروحة استكمالا لمتطلبات الحصول على درجة الماجستير في الفيزياء في كلية الدراسات العليا في جامعة النجاح الوطنية – نابلس.

2017

التمغنط لنقطة كمية منفردة من زرنخيد الغاليوم GaAs المحصورة بجهد جاوس

إعداد

محمود ماجد محمود علي

إشراف

أ.د. محمد السعيد

الملخص

قمنا بحساب التمغنط لإلكترون واحد محصور بجهد جاوس في نقطة كمية مصنوعة من مادة GaAs عن طريق حل دالة هاملتون بطريقة المحور الدقيقة اخذين بالاعتبار الحركة المغزلية للالكترون وتم فحص اعتماد كمية التمغنط على كل من المتغيرات التالية: درجة الحرارة والمجال المغناطيسي وجهد الحصر، عرضنا في هذه الاطروحة تغير طاقة الالكترون بتغيير كل من المجال المغناطيسي و شدة جهد جاوس وحجم النقطة الكمية، اظهرت المقارنات المعروضة في الاطروحة تطابقا كبيرا بين النتائج التي حصلنا عليها مع الاعمال المنشورة.